

Article

# Synthesis, Crystal Structure and DFT Studies of 1,3-Dimethyl-5-propionylpyrimidine-2,4,6(1*H*,3*H*,5*H*)-trione

Anamika Sharma <sup>1</sup>, Yahya E. Jad <sup>1</sup>, Hazem A. Ghabbour <sup>2,3</sup>, Beatriz G. de la Torre <sup>1,4</sup>, Hendrik G. Kruger <sup>1,\*</sup>, Fernando Albericio <sup>1,5,6,7,8,\*</sup> and Ayman El-Faham <sup>8,9,\*</sup>

- <sup>1</sup> School of Health Sciences, University of KwaZulu-Natal, Durban 4001, South Africa; anamika.aug14@gmail.com (A.S.); yahyajad@yahoo.com (Y.E.J.); garciadelatorreb@ukzn.ac.za (B.G.d.l.T.)
- <sup>2</sup> Department of Pharmaceutical Chemistry, College of Pharmacy, King Saud University, Riyadh 11451, Saudi Arabia; ghabbourh@yahoo.com
- <sup>3</sup> Department of Medicinal Chemistry, Faculty of Pharmacy, University of Mansoura, Mansoura 35516, Egypt
- <sup>4</sup> School of Laboratory of Medicine & Medical Sciences, University of KwaZulu-Natal, Durban 4001, South Africa
- <sup>5</sup> School of Chemistry and Physics, University of KwaZulu-Natal, Durban 4001, South Africa
- <sup>6</sup> CIBER-BBN, Networking Centre on Bioengineering, Biomaterials and Nanomedicine, Barcelona Science Park, Barcelona 08028, Spain
- <sup>7</sup> Department of Organic Chemistry, University of Barcelona, Barcelona 08028, Spain
- <sup>8</sup> Department of Chemistry, College of Science, King Saud University, P.O. Box 2455, Riyadh 11451, Saudi Arabia
- <sup>9</sup> Chemistry Department, Faculty of Science, Alexandria University, P.O. Box 426, Ibrahimia, Alexandria 12321, Egypt
- \* Correspondence: kruger@ukzn.ac.za (H.G.K.); albericio@ukzn.ac.za (F.A.); aymanel\_faham@hotmail.com (A.E.-F.); Tel.: +27-614-009-133 (F.A.)

Academic Editor: Helmut Cölfen

Received: 17 December 2016; Accepted: 16 January 2017; Published: 21 January 2017

**Abstract:** Novel 1,3-Dimethyl-5-propionylpyrimidine-2,4,6(1*H*,3*H*,5*H*)-trione was synthesized and recrystallized from ethanol. The compound was characterized by <sup>1</sup>H NMR, <sup>13</sup>C NMR in CDCl<sub>3</sub>, DMSO-*d*<sub>6</sub> and acetone-*d*<sub>6</sub>, elemental analysis and X-ray diffraction. The NMR data observed that the title compound exists in the enol tautomer rather than keto, and it stabilized by strong H-bond as observed from the NMR data at different temperatures. Theoretical calculations (DFT) were carried out using Gaussian09 program package and B3LYP correlation function. Full geometry optimization of the keto and enol forms were carried out using 6-311G++(d,p) basis set. The structure and energy of the transition state between these two tautomers were calculated. The frontier orbital energy and atomic net atomic charges of the tautomers were presented. The experimental results of the title compound have been compared with the theoretical results and it was found that the experimental data are in a good agreement with the calculated values. The transition state calculations also support the stability of enol form compared to keto form at room temperature.

**Keywords:** 1,3-dimethylpyrimidine-2,4,6-trione; X-ray; DFT molecular orbital calculations; HOMO; LUMO

## 1. Introduction

Pyrimidine-2,4,6-triones (barbiturates) belongs to the family of drugs that enhances depression of brain nerve activity producing changes in mental activity ranging from mild sedation and sleep to deep coma. Commonly, they are used to treat anxiety, insomnia, seizure disorders, migraine headaches and in surgery as general anesthetics, anticonvulsants, and anxiolytics [1–7]. Barbiturates analogs

also have recently gained significant potential as chemotherapeutic agents that have applications as antimicrobials and antifungals [8]. Other pyrimidinetrione derivatives, including bisoxadiazole and bisthiadiazole moieties, have been used as antibiotic and antifungal agents [9]. Pyrimidinetriones also belong to a broad group of drugs used as anticonvulsant, narcotic, sedative, antiepileptic, and antitumor agents [10–13]. They have found a prominent place in pharmaceutical industry because of their biochemical effects on calcium, acetylcholine, biogenic amines (Serotonin, Norepinephrine, Dopamine and Histamine), glutamate, aspartate and gamma-aminobutyric acid for the excitation-secretion coupling process involved in neurotransmitter release [14]. Recently, Donna et al. reported a number of pyrimidinetriones derivatives, including phenylhydrazones of 5-acylpyrimidinetrione that exhibited potent fungal growth inhibition with minimal mammalian cell toxicity [15]. Other derivatives possess promising therapeutic properties including anti-invasive, antiangiogenic, antiviral, central stimulant, anticancer, and calcium antagonist activities [16–18]. In view of the importance of barbiturates, we report synthesis, NMR spectra, crystal structure and theoretical calculations of 1,3-dimethyl-5-propionylpyrimidine-2,4,6(1*H*,3*H*,5*H*)-trione (Figure 1) supported by density functional theory (DFT) calculations correlating the calculated molecular orbital energies (eV) for the surfaces of the frontier molecular orbitals to the electronic excitation transitions from the absorption spectra of the title compound.

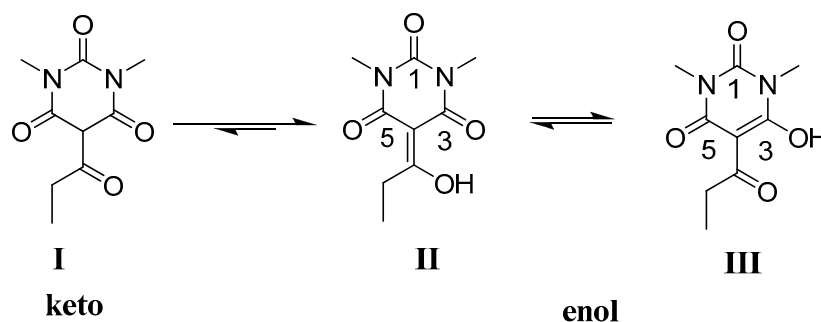


**Figure 1.** Molecular structure of title compound.

## 2. Results and Discussion

### 2.1. NMR Studies

1,3-Dimethyl-5-propionylpyrimidine-2,4,6(1*H*,3*H*,5*H*)-trione was prepared by reaction of 1,3-dimethylpyrimidine-1,3,5-trione with propionic anhydride in the presence of NaHCO<sub>3</sub> to afford the target product in yield 81%. Recently, DaSilva et al. [19] and Giziroglu et al. [20] reported that the acetyl derivative (R = CH<sub>3</sub>) exist in three tautomeric structures, as indicated in Figure 1. To select the right tautomer for the title compound, <sup>1</sup>H NMR in CDCl<sub>3</sub>, DMSO-*d*<sub>6</sub> and acetone-*d*<sub>6</sub> was checked. The <sup>1</sup>H NMR in CDCl<sub>3</sub> (Figure S2, Supplementary Materials) showed triplet peak at δ = 1.21 and 3.16 related to the ethyl group, two singlet peaks at δ = 3.32 and 3.36 corresponding, the two N-CH<sub>3</sub> and a singlet peak at 17.61 for the enolic OH. <sup>13</sup>C NMR (Figure S3, Supplementary Materials) showed peaks at δ = 9.4 and 27.9 for the ethyl group and one peak at δ = 30.4 for the two N-CH<sub>3</sub>, the peak at δ = 94.9 for the C=C-OH, while the other peaks are related to the three carbonyl groups at δ = 150.4 (C1), 160.8 (C5), 169.9 (C<sub>2</sub>H<sub>5</sub>-CO), and at δ = 200.6 (C=C-OH, enolic carbon). This observation is in a good agreement with structure III (Figure 1).

Then, we checked the <sup>1</sup>H NMR in DMSO-*d*<sub>6</sub> (Figure S5, Supplementary Materials), and observed that the spectral data were slightly different compared to in CDCl<sub>3</sub>, where the <sup>1</sup>H NMR showed triplet peak at δ = 1.14 and quartet peak at δ = 3.12 related CH<sub>3</sub>-CH<sub>2</sub>, one singlet peak at δ = 3.18 for the two N-CH<sub>3</sub> and a singlet peak at δ 17.62 for the enolic OH. The <sup>13</sup>C NMR (Figure S6, Supplementary Materials) showed peaks at δ = 9.8 and 28.1 for the ethyl group (CH<sub>3</sub>-CH<sub>2</sub>) and one peak at δ 30.1 for the two methyl (N-CH<sub>3</sub>), the peak at δ = 95.4 for the C=C-OH, one peak at δ = 150.5 for C1 (C-CO-C),

one peak at  $\delta = 161.1$  for the carbon (C3 and C5), and finally one peak at  $\delta = 199.4$  related to the enolic carbon (C=C-OH). This observation is also in good agreement with the proposed structure II. The  $^1\text{H}$  NMR in acetone (Figure S4, Supplementary Materials) showed the same observation as in case of DMSO. To check the effect of temperature on the stability of the proposed structure,  $^1\text{H}$  NMR in DMSO at 20 °C, 30 °C and 40 °C (Figures S5, S7 and S8, Supplementary Materials) was also observed. The spectral data did not change except that the peaks at 17.6 became broader. This means that the enol form is stabilized by strong H-bond, and the obtained results agreed with the reported data for the aroylhydrazone derivatives of 1,3-dimethyl-5-acetylbarbituric acid reported by DaSilva and others [19,20]. Finally, the NMR data obtained explain that this type of compound exists in solution in the enol form and the structure of the enol depends on the type and polarity of the solvent use as it is stabilized by presence of strong intra-molecular hydrogen bond which was further confirmed by X-ray spectroscopy.

## 2.2. X-ray Structural Study and Theoretical Calculations

$^1\text{H}$  NMR of the title compound showed presence of -OH proton at  $\delta = 17.61$  (singlet) confirming more stability of enol form compared to keto form. The same tautomeric structure was also observed in the solid state by X-ray diffraction. The asymmetric unit contains one independent molecule according to crystal packing that is shown in Figure 2 (Table S1, Supplementary Materials). It was found to crystallize in  $P2_1/C$  space group. Bond lengths are in normal ranges [21], as shown in Table 1. The crystal packing reveals that the title compound is planar. In addition, the O4-C7 bond length is found to be 1.310 (2), which is larger than normal C=O double bond (1.21 Å). It is also less than standard C-O single bond (1.432 Å) [21]. The bond length of C5=O3 is 1.264 (3), longer than other keto bonds C1=O1 and C3=O2 in the same structure, because this carbonyl bond is proton acceptor and thus weakened by the intra-molecular hydrogen bond. H1O4 makes strong intra-molecular hydrogen bond with O3 as explained in Figure 2. This intra-molecular hydrogen bond stabilizes the enol form more than keto. Further, intermolecular  $\pi$ - $\pi$  stacking interaction can be observed C1-C5 (3.373 Å both length) as shown in the packing diagram (Figure 2). In addition, a weak intermolecular interaction is observed between C5-O1 and C1-H of N2 with bond lengths of 2.958 Å and 2.758 Å, respectively.

**Table 1.** Selected bond lengths (Å), angles (°) and theoretical calculations for the title compound.

Bond Lengths	X-ray Crystal	DFT <sup>a</sup>	Bond Angles	X-ray Crystal	DFT <sup>a</sup>
O1-C1	1.218 (2)	1.2215	C2-N1-C3	116.2 (2)	115.6509
O2-C3	1.213 (3)	1.2142	C1-N1-C2	118.14 (17)	118.7543
O3-C5	1.264 (3)	1.2489	C1-N1-C3	125.7 (2)	125.5948
O4-C7	1.310 (3)	1.3082	C3-N2-C4	117.76 (19)	118.4499
N1-C1	1.404 (3)	1.4113	C3-N2-C5	123.31 (17)	123.7613
N1-C2	1.476 (3)	1.4706	C4-N2-C5	118.90 (19)	117.7888
N1-C3	1.383 (3)	1.3878	O1-C1-N1	119.39 (18)	119.8531
N2-C3	1.391 (3)	1.4038	N1-C1-C6	115.03 (17)	115.4104
N2-C5	1.372 (3)	1.3781	O1-C1-C6	125.58 (19)	124.7364
N2-C4	1.472 (3)	1.4708	O2-C3-N2	121.34 (18)	121.7422
			N1-C3-N2	116.6 (2)	116.5854
			O2-C3-N1	122.0 (2)	121.6725
			N2-C5-C6	119.07 (18)	118.5093
			O3-C5-N2	118.04 (18)	118.5799
			O3-C5-C6	122.88 (19)	122.9107
			O4-C7-C6	119.18 (18)	120.1114
			O4-C7-C8	115.04 (17)	114.6609

<sup>a</sup> B3LYP/6-311++G(d,p). Cartesian coordinates of all optimized structures are provided in the Supplementary Materials.

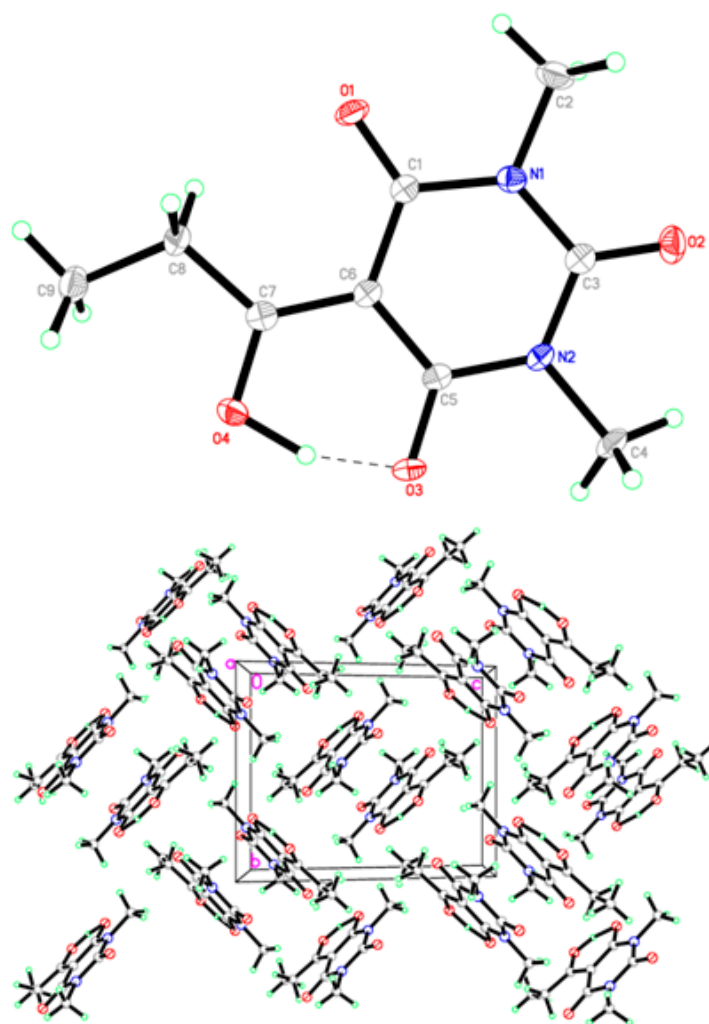


Figure 2. Asymmetric unit and crystal packing in title compound.

A density functional theory (DFT) geometry optimization with the Gaussian09 program package [22] employing the B3LYP (Becke three parameters Lee–Yang–Parr exchange correlation functional, which combines the hybrid exchange functional of Becke [23] with the gradient-correlation functional of Lee, Yang and Parr [24] and the 6-311G++(d,p) basis set were performed in gas phase). No solvent corrections were made with these calculations as it was reported that gas phase calculations frequently correspond quite well with crystal structures [25]. Starting geometries were taken from X-ray refined data. The optimized geometry results in the free molecule state were compared to those in the crystalline state (Table S2, Supplementary Materials). No negative vibrational modes were obtained. The DFT calculated structure and geometric parameters (bond lengths and bond angles) are given in Table 1 (Figure S1, Supplementary Materials). All optimized structures have C1 point group. The optimized C19–O4 bond length is 1.308 Å (experimentally found 1.310 Å), which is more representative of a single bond (other C=O bonds are 1.22 Å) and H27–O4 makes strong intra-molecular hydrogen bond with O3.

### 2.3. Frontier Orbital Energy Analysis and Molecular Total Energies

Molecular Total Energy and Frontier Orbital energy levels are calculated using DFT (Table 2).

**Table 2.** Total energy and frontier orbital energy (B3LYP/6-311++G(d,p)).

	DFT (Enol Form)	DFT (Keto Form)
$E_{\text{total}}^a$	−760.87486944	−760.84960093
$E_{\text{HOMO}}$	−0.27058	−0.27366
$E_{\text{LUMO}}$	−0.07757	−0.06897
$\Delta E^b$	0.19301	0.20469

<sup>a</sup> 1 Hartree =  $4.35974417 \times 10^{-18}$  J = 27.2113845 eV; <sup>b</sup>  $\Delta E = E_{\text{LUMO}} - E_{\text{HOMO}}$ . (Cartesian coordinates of all optimized structures are provided with the Supplementary Materials).

The geometry of the title compound was optimized using DFT method in the gas phase. The crystal structure of title compound (enol form) was used for DFT studies. The energy gap between HOMO and LUMO was calculated by B3LYP method using 6-311G++(d,p) basis set. The title compound (in enol form) shows energy gap ( $\Delta E = 0.19464$  Hartree = 5.25 eV) for HOMO  $\rightarrow$  LUMO (Figure 3). The keto form was optimized using GaussView05 [26] and the results were compared with that of enol form, as shown in Table 2. The keto form shows energy gap ( $\Delta E = 0.20469$  Hartree = 5.57 eV) for HOMO  $\rightarrow$  LUMO, which is higher than that of enol form.

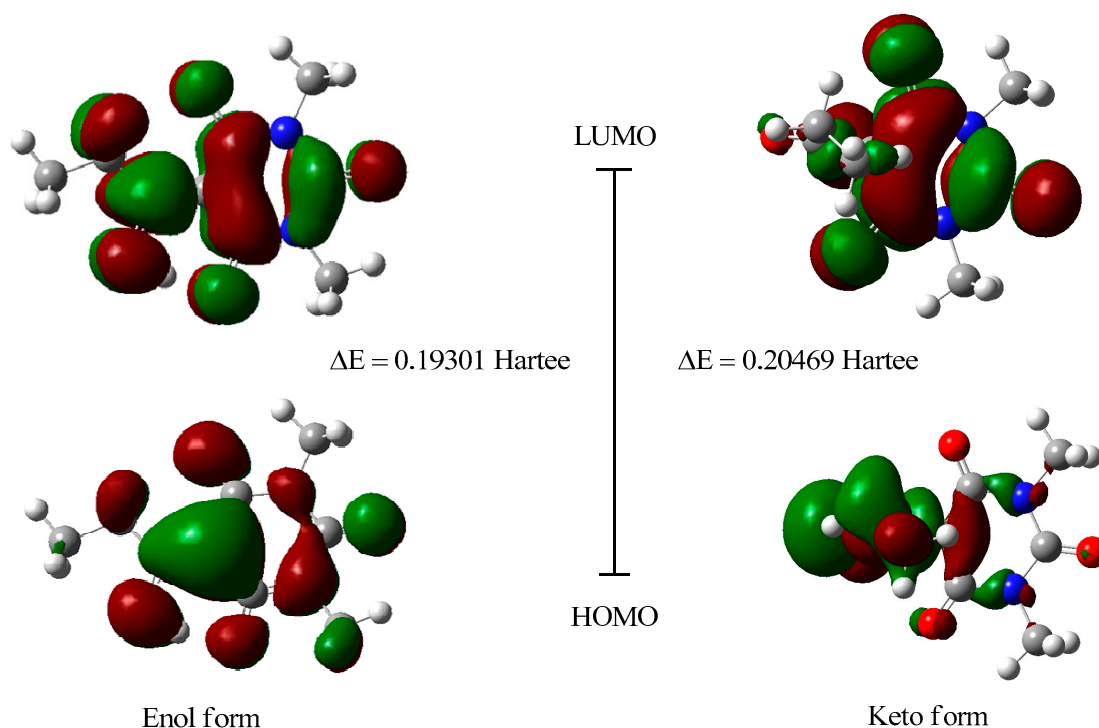


**Figure 3.** Frontier molecular orbital's of title compound (B3LYP/6-311++G(d,p)) (Cartesian coordinates of all optimized structures are provided in the Supplementary Materials).

The HOMO and LUMO are important factors that affect the bioactivity, chemical reactivity, electron affinity and ionization potential [27–32]. Thus, study of the frontier orbital energy can provide useful information about the biological and chemical reaction mechanism.

#### 2.4. Transition State Calculations

A transition state is a first order saddle point on the Potential Energy Surface (PES) of the molecular system. The vibrational spectrum of a transition state is characterized by one imaginary frequency (implying a negative force constant), which means that in one direction in nuclear configuration space the energy has a maximum, while in all other orthogonal directions the energy is a minimum [33].

To verify this, keto form of the title compound was optimized using Gaussian09. The optimized geometry was used to perform frequency calculations at the same computational level (Table S3, Supplementary Materials). Molecules have enough thermal and kinetic energy at room temperature to allow processes requiring between 15 and 20 kcal/mol [34]. The calculated energies are tabulated in Table 3 and shown schematically in Figure 4. The calculated energy confirms that the reaction (Figure 1) is more favorable in enol form. To convert the keto form to the enol, an energy barrier of 55.47 kcal/mol needs to be overcome (Table S4, Supplementary Materials); this is much higher than the inherent energy of 15–20 kcal/mol limit at room temperature [35,36]. Hence, the theoretical results suggest that if the product (enol) is formed, it will not interconvert at room temperature. This is confirmed by the NMR spectra (only enol form is observed).

**Table 3.** Calculated reaction profile using DFT (B3LYP/6-311++G(d,p)).

	Relative Energies (kcal/mol)
Keto form	0
Transition State	40.54
Enol form	−14.93

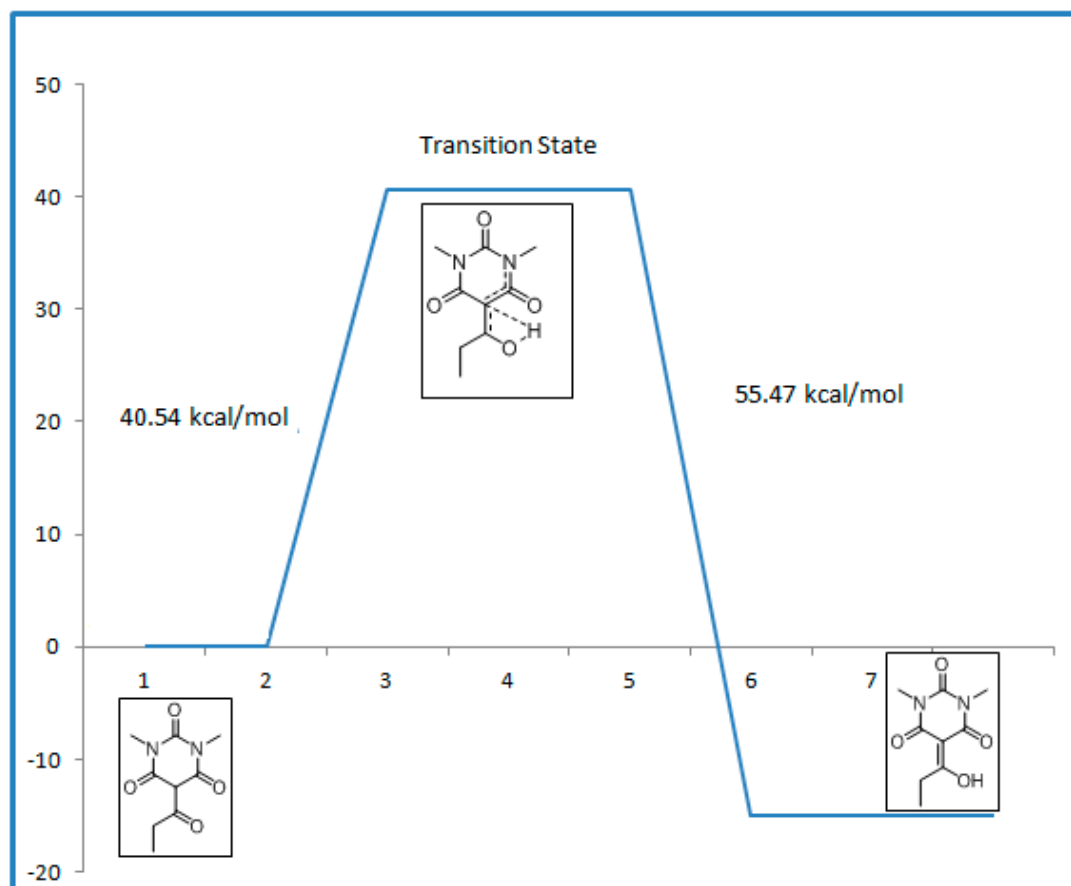


**Figure 4.** Transition state for keto–enol form of title compound.

### 3. Materials and Methods

#### 3.1. General

1,3-dimethylpyrimidine-2,4,6-trione and acetic anhydride were purchased from Sigma-Aldrich (Sigma-Aldrich Chemie GmbH, 82024 Taufkirchen, Germany). The solvents used were of analytical

and HPLC reagent grade. Melting points were determined with a Mel-Temp apparatus and are uncorrected (Sigma-Aldrich Chemie GmbH, 82024 Taufkirchen, Germany). Magnetic resonance spectra ( $^1\text{H}$  NMR and  $^{13}\text{C}$  NMR spectra) recorded on a JEOL 400 and 500 MHz spectrometer (JEOL, Ltd., Tokyo, Japan) with chemical shift values reported in  $\delta$  units (ppm). Elemental analyses were performed on Perkin-Elmer 2400 elemental analyzer (PerkinElmer, Inc., 940 Winter Street, Waltham, MA, USA), and the values found were within  $\pm 0.3\%$  of the theoretical values.

### 3.2. General Procedure

1,3-dimethylpyrimidine-2,4,6-trione (50 mmol) was suspended in very small amount of water and a concentrated water solution of sodium bicarbonate ( $\text{NaHCO}_3$ , 50 mmol) was added. After gas evolution ceased, propionic anhydride (5 eq.) was added to the stirred solution. A white precipitate formed after about 5 min. The mixture was stirred overnight and then the white precipitate was filtered, and the precipitate dissolved in 15% ammonium hydroxide ( $\text{NH}_4\text{OH}$ ). Hydrochloric acid ( $\text{HCl}$ ) was added until pH was below 1; the temperature of the solution rose and the precipitate formed was filtered and allowed to dry at room temperature. The solid was recrystallized from ethanol which afforded white crystals in yield 81%. m.p. = 55–56 °C;

$^1\text{H}$  NMR (400 MHz,  $\text{CDCl}_3$ )  $\delta$  = 1.21 (t, 3H,  $J$  = 6.8 MHz,  $\text{CH}_3$ ), 3.15 (q, 2H,  $J$  = 7.2 MHz,  $\text{CH}_2$ ), 3.32 (s, 3H,  $\text{CH}_3$ ), 3.36 (s, 3H,  $\text{CH}_3$ ), 17.61 (s, 1H, OH);  $^{13}\text{C}$  NMR (100 MHz,  $\text{CDCl}_3$ )  $\delta$  = 9.4, 27.9, 30.4, 94.9, 150.4, 160.8, 169.7, 200.6; Anal. Calcd for  $\text{C}_9\text{H}_{12}\text{N}_2\text{O}_4$  (212.21): C, 50.94; H, 5.70; N, 13.20; Found: C, 51.12; H, 5.81; N, 13.01.

$^1\text{H}$  NMR (500 MHz,  $\text{DMSO}-d_6$ )  $\delta$  = 1.14 (t, 3H,  $J$  = 8.0 MHz,  $\text{CH}_3$ ), 3.09 (q, 2H,  $J$  = 9.5 MHz,  $\text{CH}_2$ ), 3.18 (s, 6H, 2 $\text{CH}_3$ ), 17.62 (brs, 1H, OH);  $^{13}\text{C}$  NMR (125 MHz,  $\text{DMSO}-d_6$ )  $\delta$  = 9.8 ( $\text{CH}_3$ ), 28.1 ( $\text{CH}_2$ ), 30.1 (2 N- $\text{CH}_3$ ), 95.4 ( $\text{C}=\text{C}-\text{OH}$ ), 150.4 (N-CO-N), 161.1 (N-CO-C=), 199.4 ( $\text{C}=\text{C}-\text{OH}$ ).

### 3.3. Structure Determination

The title compound was obtained as single crystal by slow evaporation from ethanol solution of the pure compound at room temperature. Data were collected on a Bruker APEX-II D8 Venture area diffractometer, equipped with graphite monochromatic Mo  $K\alpha$  radiation,  $\lambda$  = 0.71073 Å at 100 (2) K. Cell refinement and data reduction were carried out by Bruker SAINT. SHELXS [37,38] was used to solve structure. The final refinement was carried out by full-matrix least-squares techniques with anisotropic thermal data for nonhydrogen atoms on  $f$ . CCDC 1438344 contains the supplementary crystallographic data for this compound can be obtained free of charge from the Cambridge Crystallographic Data Centre via [www.ccdc.cam.ac.uk/data\\_request/cif](http://www.ccdc.cam.ac.uk/data_request/cif).

### 3.4. Theoretical Calculations

According to the above crystal structure, a crystal unit was selected as the initial structure, while DFT-B3LYP/6-311G++(d,p) methods in Gaussian09 [22] was used to optimize the structure of the title compound. No solvent corrections were made with these calculations. Vibration analysis showed that the optimized structure indeed represents a minimum on the potential energy surface (no negative eigenvalues). A four-membered ring transition state was calculated. The transition state was also confirmed using IRC [39,40] calculations. The Cartesian coordinates of all optimized structures are provided in the Supplementary Materials.

## 4. Conclusions

In conclusion, 1,3-dimethyl-5-propionylpyrimidine-2,4,6(1H,3H,5H)-trione was synthesized and characterized by  $^1\text{H}$  NMR,  $^{13}\text{C}$  NMR, elemental analysis and X-ray single diffraction. X-ray structure of title compound shows bond length between O4-C7 as 1.310 (2), which is larger than normal C-O double bond. In addition, formation of strong intramolecular bond takes place between H1O4 and O3, which clearly indicates more stability for enol form compared to keto form. The experimental data were

co-related with DFT theoretical calculations using B3LYP/6-311G++(d,p) basis set. The experimental data are well supported by theoretical studies that clearly indicate stability of enol form compared to keto form. The transition state calculations also confirm the stability of enol form, as an energy barrier of 55.47 kcal/mol (which is much higher than 15 kcal/mol) is required to form keto form. Hence, the title compound crystallizes in more stable enol form.

**Supplementary Materials:** The following are available online at [www.mdpi.com/2073-4352/7/1/31/s1](http://www.mdpi.com/2073-4352/7/1/31/s1), Table S1: The calculated bond distances and bond angles compared to the experimental data of title compound; Table S2: Optimized Cartesian Coordinates (Å) of enol form for title compound; Table S3: Optimized Cartesian Coordinates (Å) of keto form for title compound; Table S4: Optimized Cartesian Coordinates (Å) for calculation of transition state; Figure S1: Optimized geometry of the title compound [B3LYP/6-311++G(d,p)]; Figure S2: <sup>1</sup>H NMR of title compound in CDCl<sub>3</sub>; Figure S3: <sup>13</sup>C NMR of title compound in CDCl<sub>3</sub>; Figure S4: <sup>1</sup>H NMR of title compound in acetone-*d*<sub>6</sub>; Figure S5: <sup>1</sup>H NMR of title compound in DMSO-*d*<sub>6</sub> at 20 °C; Figure S6: <sup>13</sup>C NMR of title compound in DMSO-*d*<sub>6</sub> at 20 °C; Figure S7: <sup>1</sup>H NMR of title compound in DMSO-*d*<sub>6</sub> at 30 °C; Figure S8: <sup>1</sup>H NMR of title compound in DMSO-*d*<sub>6</sub> at 40 °C.

**Acknowledgments:** This work was funded in part by the following: National Research Foundation (NRF) and the University of KwaZulu-Natal (South Africa); International Scientific Partnership Program ISPP at King Saud University (ISPP# 0061) (Saudi Arabia); and MEC (CTQ2015-67870-P), Generalitat de Catalunya (2014 SGR 137) (Spain).

**Author Contributions:** Anamika Sharma and Hendrik G. Kruger performed D.F.T. theoretical calculations. Ayman El-Faham carried out the synthesis, designed the proposed methods, and analyzed the data together with Yahya E. Jad, Beatriz G. de la Torre, and Fernando Albericio. Hazem A. Ghabbour carried out X-ray and characterization. All authors contributed to the preparation of the manuscript.

**Conflicts of Interest:** The authors declare no conflict of interest.

## References

1. Goodman, L.; Gilman, A. *The Pharmacological Basis of Therapeutics*; McGraw-Hill: New York, NY, USA, 1996; pp. 959–975.
2. Olin, B. *Central Nervous System Drugs, Sedatives and Hypnotics, Barbiturates, in Fact and Comparisons Drug Information*; Facts and Comparisons: St. Louis, MO, USA, 1993; pp. 1398–1413.
3. Brunton, L.; Lazo, J.; Parker, K.G. *Gilman's the Pharmacological Basis of Therapeutics*, 11th ed.; Mc Graw-Hill: New York, NY, USA, 2005.
4. Johns, M. Sleep and hypnotic drugs. *Drugs* **1975**, *9*, 448–478. [[CrossRef](#)] [[PubMed](#)]
5. Whittle, S.R.; Turner, A.J. Differential effects of sedative and anticonvulsant barbiturates on specific [3 h] gaba binding to membrane preparations from rat brain cortex. *Biochem. Pharmacol.* **1982**, *31*, 2891–2895. [[CrossRef](#)]
6. Brunner, H.; Ittner, K.P.; Lunz, D.; Schmatloch, S.; Schmidt, T.; Zabel, M. Highly enriched mixtures of methohexital stereoisomers by palladium-catalyzed allylation and their anaesthetic activity. *Eur. J. Org. Chem.* **2003**, *2003*, 855–862. [[CrossRef](#)]
7. Lyons, K.E.; Pahwa, R. Pharmacotherapy of essential tremor. *CNS Drugs* **2008**, *22*, 1037–1045. [[CrossRef](#)] [[PubMed](#)]
8. Padmaja, A.; Reddy, G.S.; Venkata Nagendra Mohan, A.; Padmavathi, V. Michael adducts-source for biologically potent heterocycles. *Chem. Pharm. Bull.* **2008**, *56*, 647–653. [[CrossRef](#)] [[PubMed](#)]
9. Padmavathi, V.; Reddy, G.D.; Venkatesh, B.C.; Padmaja, A. One-pot synthesis of 5-[[bis (azolylmethylthio)]methylene] pyrimidine-2,4,6-(1H,3H,5H)-triones. *Arch. Pharm.* **2011**, *344*, 165–169. [[CrossRef](#)] [[PubMed](#)]
10. Uhlmann, C.; Fröscher, W. Low risk of development of substance dependence for barbiturates and clobazam prescribed as antiepileptic drugs: Results from a questionnaire study. *CNS Neurosci. Ther.* **2009**, *15*, 24–31. [[CrossRef](#)] [[PubMed](#)]
11. Maquoi, E.; Sounni, N.E.; Devy, L.; Olivier, F.; Frankenne, F.; Krell, H.-W.; Grams, F.; Foidart, J.-M.; Noël, A. Anti-invasive, antitumoral, and antiangiogenic efficacy of a pyrimidine-2,4,6-trione derivative, an orally active and selective matrix metalloproteinases inhibitor. *Clin. Cancer Res.* **2004**, *10*, 4038–4047. [[CrossRef](#)] [[PubMed](#)]

12. Breyholz, H.J.; Wagner, S.; Faust, A.; Riemann, B.; Höltke, C.; Hermann, S.; Schober, O.; Schäfers, M.; Kopka, K. Radiofluorinated pyrimidine-2,4,6-triones as molecular probes for noninvasive mmp-targeted imaging. *ChemMedChem* **2010**, *5*, 777–789. [[CrossRef](#)] [[PubMed](#)]
13. Bartsch, P.; Cataldo, D.; Endelev, R.; Evrard, B.; Foidart, J.M.; Krell, H.W.; Zimmermann, G. Cyclodextrin Inclusions Complexes of Pyrimidine-2,4,6-Triones. Google Patents WO2005097058 A3, 17 August 2006.
14. Richter, J.A.; Holtman, J.R. Barbiturates: Their in vivo effects and potential biochemical mechanisms. *Prog. Neurobiol.* **1982**, *18*, 275–319. [[CrossRef](#)]
15. Neumann, D.M.; Cammarata, A.; Backes, G.; Palmer, G.E.; Jursic, B.S. Synthesis and antifungal activity of substituted 2,4,6-pyrimidinetrione carbaldehyde hydrazones. *Biorg. Med. Chem.* **2014**, *22*, 813–826. [[CrossRef](#)] [[PubMed](#)]
16. Katritzky, A.R.; Rees, C.W. *Comprehensive Heterocyclic Chemistry*; Pergamon Press: Oxford, UK, 1984.
17. Perspicace, E.; Jouan-Hureauux, V.; Ragno, R.; Ballante, F.; Sartini, S.; La Motta, C.; Da Settimo, F.; Chen, B.; Kirsch, G.; Schneider, S. Design, synthesis and biological evaluation of new classes of thieno [3,2-*d*] pyrimidinone and thieno [1,2,3] triazine as inhibitor of vascular endothelial growth factor receptor-2 (vegfr-2). *Eur. J. Med. Chem.* **2013**, *63*, 765–781. [[CrossRef](#)] [[PubMed](#)]
18. Nie, Z.; Perretta, C.; Erickson, P.; Margosiak, S.; Almassy, R.; Lu, J.; Averill, A.; Yager, K.M.; Chu, S. Structure-based design, synthesis, and study of pyrazolo [1,5-*a*][1,3,5] triazine derivatives as potent inhibitors of protein kinase ck2. *Biorg. Med. Chem. Lett.* **2007**, *17*, 4191–4195. [[CrossRef](#)] [[PubMed](#)]
19. Da Silva, E.T.; Lima, E.L. Reaction of 1,3-dimethyl-5-acetyl-barbituric acid (dab) with primary amines. Access to intermediates for selectively protected spermidines. *Tetrahedron Lett.* **2003**, *44*, 3621–3624. [[CrossRef](#)]
20. Giziroglu, E.; Aygün, M.; Sarikurcu, C.; Kazar, D.; Orhan, N.; Firinci, E.; Soyleyici, H.C.; Gokcen, C. Synthesis, characterization and antioxidant activity of new dibasic tridentate ligands: X-ray crystal structures of dmsu adducts of 1,3-dimethyl-5-acetyl-barbituric acid o-hydroxybenzoyl hydrazone copper (ii) complex. *Inorg. Chem. Commun.* **2013**, *36*, 199–205. [[CrossRef](#)]
21. Allen, F.H.; Kennard, O.; Watson, D.G.; Brammer, L.; Orpen, A.G.; Taylor, R. Tables of bond lengths determined by X-ray and neutron diffraction. Part 1. Bond lengths in organic compounds. *J. Chem. Soc. Perkin Trans.* **1987**, *2*, S1–S19. [[CrossRef](#)]
22. Frisch, M.J.; Trucks, G.W.; Schlegel, H.B.; Scuseria, G.E.; Robb, M.A.; Cheeseman, J.R.; Scalmani, G.; Barone, V.; Mennucci, B.; Petersson, G.A.; et al. *Gaussian 09*; Gaussian, Inc.: Wallingford, CT, USA, 2009.
23. Becke, A.D. Density-functional exchange-energy approximation with correct asymptotic behavior. *Phys. Rev. A* **1988**, *38*, 3098. [[CrossRef](#)]
24. Lee, C.; Yang, W.; Parr, R.G. Development of the colle-salvetti correlation-energy formula into a functional of the electron density. *Phys. Rev. B* **1988**, *37*, 785. [[CrossRef](#)]
25. Honarparvar, B.; Govender, T.; Maguire, G.E.; Soliman, M.E.; Kruger, H.G. Integrated approach to structure-based enzymatic drug design: Molecular modeling, spectroscopy, and experimental bioactivity. *Chem. Rev.* **2013**, *114*, 493–537. [[CrossRef](#)] [[PubMed](#)]
26. Dennington, R.; Keith, T.; Millam, J. *Gaussview*, version 5; Semichem Inc.: Shawnee Missions, KS, USA, 2009.
27. Contreras, R.; Domingo, L.R.; Andrés, J.; Pérez, P.; Tapia, O. Nonlocal (pair site) reactivity from second-order static density response function: Gas-and solution-phase reactivity of the acetaldehyde enolate as a test case. *J. Phys. Chem. A* **1999**, *103*, 1367–1375. [[CrossRef](#)]
28. Clare, B.W. Frontier orbital energies in quantitative structure-activity relationships: A comparison of quantum chemical methods. *Theor. Chim. Acta* **1994**, *87*, 415–430. [[CrossRef](#)]
29. Clare, B.W. The relationship of charge transfer complexes to frontier orbital energies in qsar. *J. Mol. Struct. Theochem.* **1995**, *331*, 63–78. [[CrossRef](#)]
30. Clare, B.W. Charge transfer complexes and frontier orbital energies in qsar: A congeneric series of electron acceptors. *J. Mol. Struct. Theochem.* **1995**, *337*, 139–150. [[CrossRef](#)]
31. Heaton, C.; Miller, A.; Powell, R. Predicting the reactivity of fluorinated compounds with copper using semi-empirical calculations. *J. Fluor. Chem.* **2001**, *107*, 1–3. [[CrossRef](#)]
32. Zhang, G.; Musgrave, C.B. Comparison of DFT methods for molecular orbital eigenvalue calculations. *J. Phys. Chem. A* **2007**, *111*, 1554–1561. [[CrossRef](#)] [[PubMed](#)]
33. Lewars, E. The concept of the potential energy surface. In *Computational Chemistry: Chapter 2—Introduction to the Theory and Applications of Molecular and Quantum Mechanics*; Springer: Boston, MA, USA, 2003; pp. 9–41.
34. Hendrickson, J.; Cram, D. *Gs Hammond Organic Chemistry*; McGraw-Hill: New York, NY, USA, 1970.

35. Kruger, H.G. Ab initio mechanistic study of the protection of alcohols and amines with anhydrides. *J. Mol. Struct. Theochem.* **2002**, *577*, 281–285. [[CrossRef](#)]
36. Singh, T.; Kruger, H.G.; Bisetty, K.; Power, T.D. Theoretical study on the formation of a pentacyclo-undecane cage lactam. *Comput. Theor. Chem.* **2012**, *986*, 63–70. [[CrossRef](#)]
37. Sheldrick, G.M. A short history of shelx. *Acta Crystallogr. Sect. A Found. Crystallogr.* **2008**, *64*, 112–122. [[CrossRef](#)] [[PubMed](#)]
38. Sheldrick, G.M. *SHELXTL-PC (Version 5.1)*; Siemens Analytical Instruments, Inc.: Madison, WI, USA, 1997.
39. Gonzalez, C.; Schlegel, H.B. An improved algorithm for reaction path following. *J. Chem. Phys.* **1989**, *90*, 2154–2161. [[CrossRef](#)]
40. Gonzalez, C.; Schlegel, H.B. Reaction path following in mass-weighted internal coordinates. *J. Phys. Chem.* **1990**, *94*, 5523–5527. [[CrossRef](#)]



© 2017 by the authors; licensee MDPI, Basel, Switzerland. This article is an open access article distributed under the terms and conditions of the Creative Commons Attribution (CC BY) license (<http://creativecommons.org/licenses/by/4.0/>).